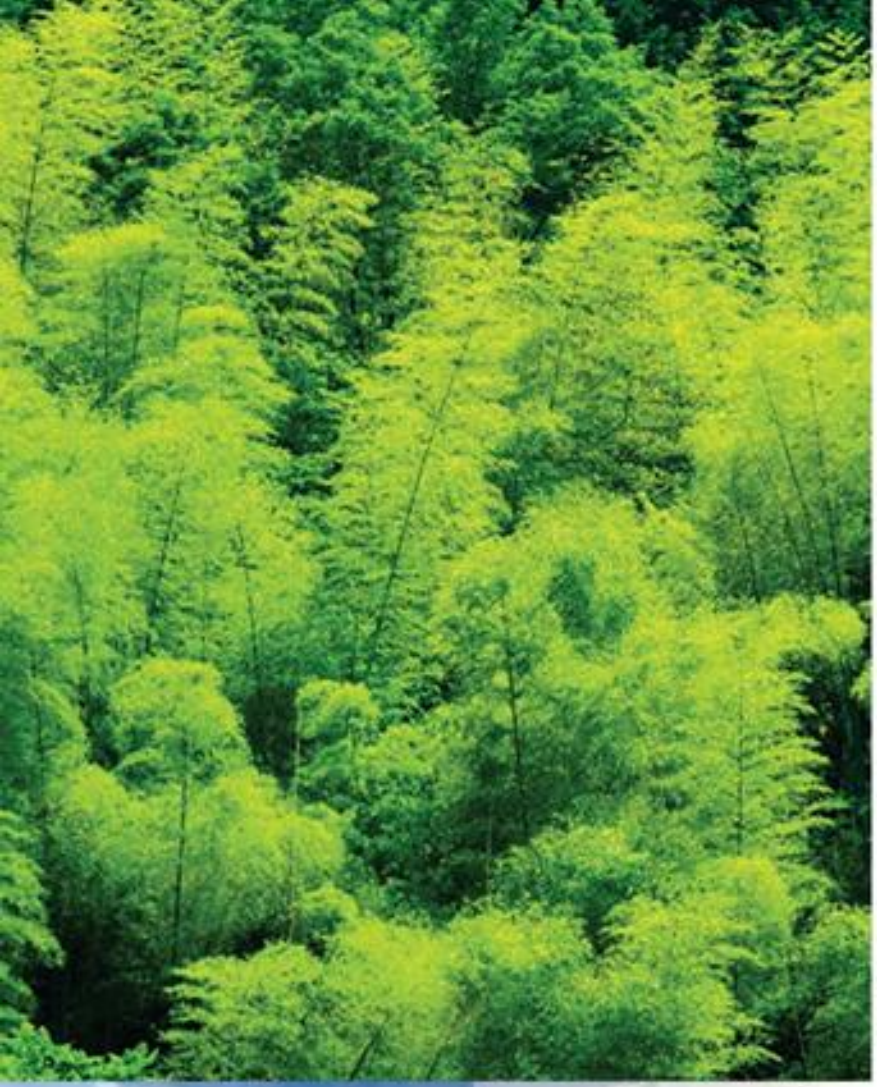

"*Role of Induced and Natural Imbibition in Frac Fluid Transport and Fate in Gas Shales*"

Alan P. Byrnes
Chief Petrophysicst

Technical Workshops for Hydraulic Fracturing Study
Fate & Transport · March 28-29, 2011
US EPA Conference Center
One Potomac Yard (South Building)
2777 S. Crystal Drive
Arlington, VA 22202 Room S-4370 and 4380

Chesapeake Energy Corporation
6100 N. Western Avenue ı Oklahoma City, OK 76118 ı 405-935-8000
AskChesapeake@chk.com ı chk.com ı NYSE: CHK

Overview

- Hydraulic fracture (HF) models & production decay analysis support estimates of propped HF surface areas of 12 $*10^6$ sq ft and created area of 24-60 $*10^6$ sq ft.
- Frac fluid 30±10% recovered/70±10% leaks off into the fracture face
- Elevated frac fluid saturations within 2 – 6 inches of the frac face.
- High capillary pressures in shales
- High frac-face Sw is not in equilibrium and capillary forces act to imbibe the fluid into the reservoir away from the frac face
- Frac fluids imbibed into the formation are effectively locked in place by capillary pressure forces of hundreds to thousands of pounds per square inch (psi) both during the life of the well production and for geologic periods of time after reservoir depletion

CHK's Operating Areas

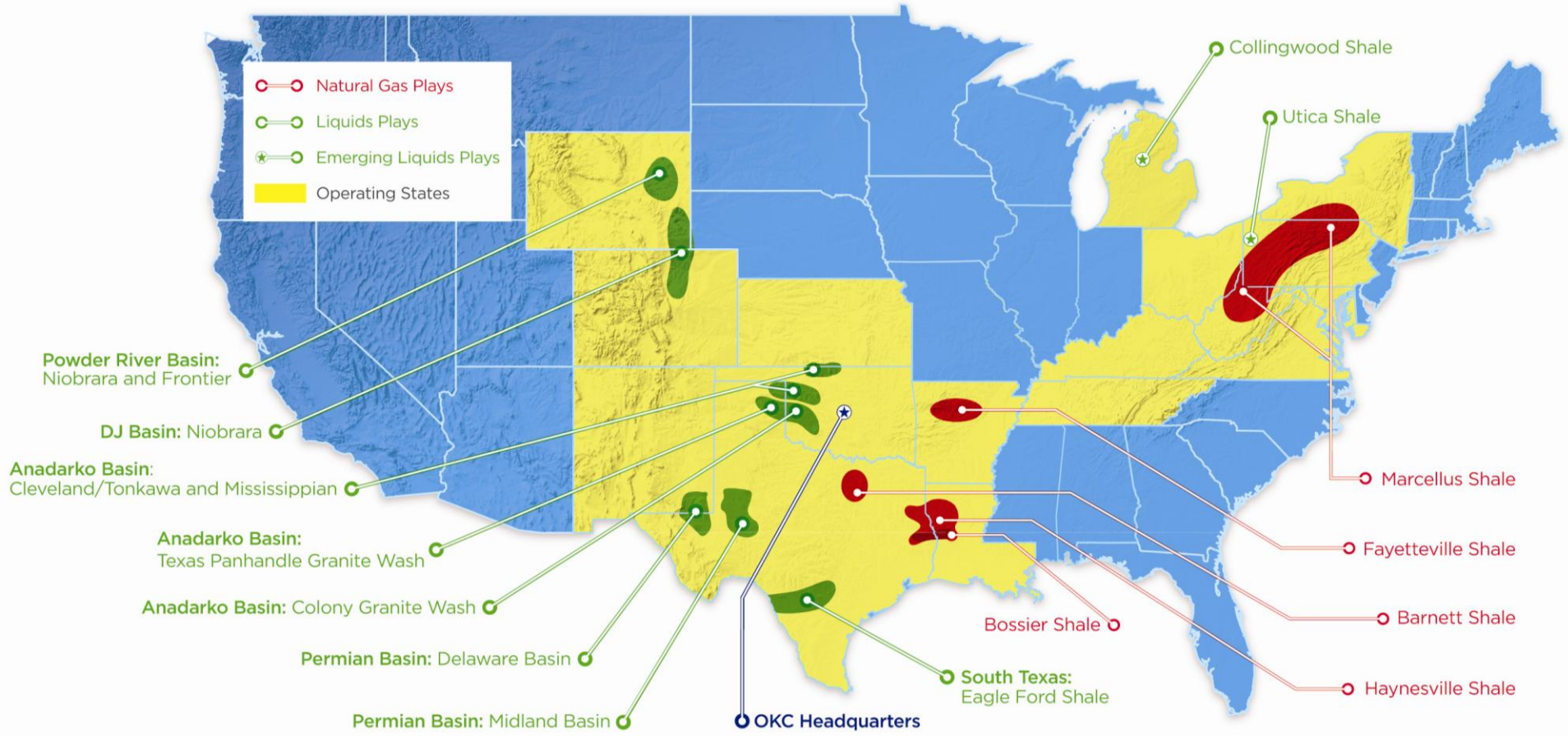

Low-risk, U.S. onshore asset base; Not exposed to economic, geopolitical or technological risks internationally or in the Gulf of Mexico

Fate and Transport Issues

- Basic Parameters
  - Time: Near-term, Long-term
  - Location: Reservoir, Wellbore, Surface
  - Substance: Gas, Liquid(s)

Time	Location	Substance
Near-term	Surface	Gas
Near-term	Surface	Liquid
Near-term	Wellbore	Gas
Near-term	Wellbore	Liquid
Near-term	Reservoir	Gas
Near-term	Reservoir	Liquid

Time	Location	Substance
Long-term	Surface	Gas
Long-term	Surface	Liquid
Long-term	Wellbore	Gas
Long-term	Wellbore	Liquid
Long-term	Reservoir	Gas
Long-term	Reservoir	Liquid

- This talk will focus on near- and long-term fate and transport of liquids in the reservoir (and wellbore)

Fracture Fluids & Proppant

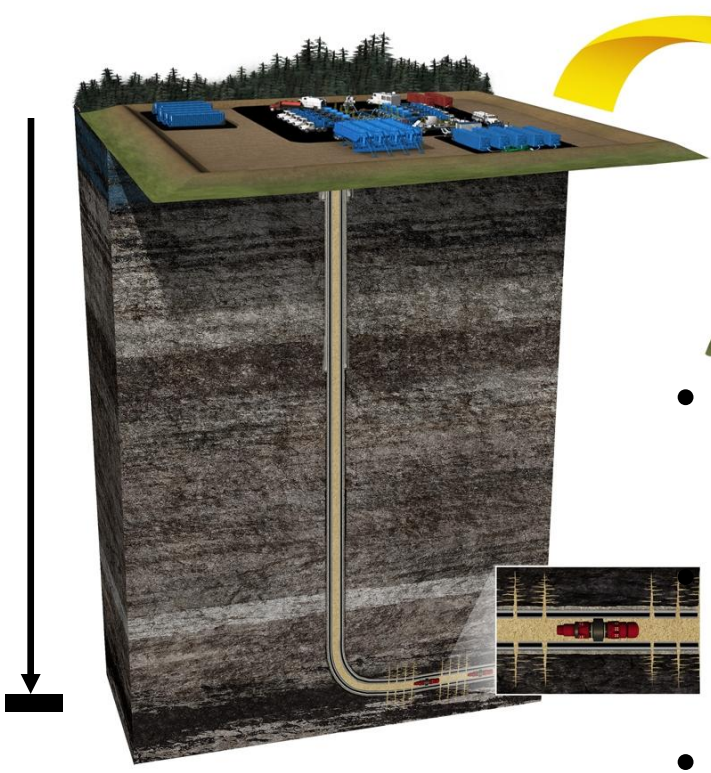

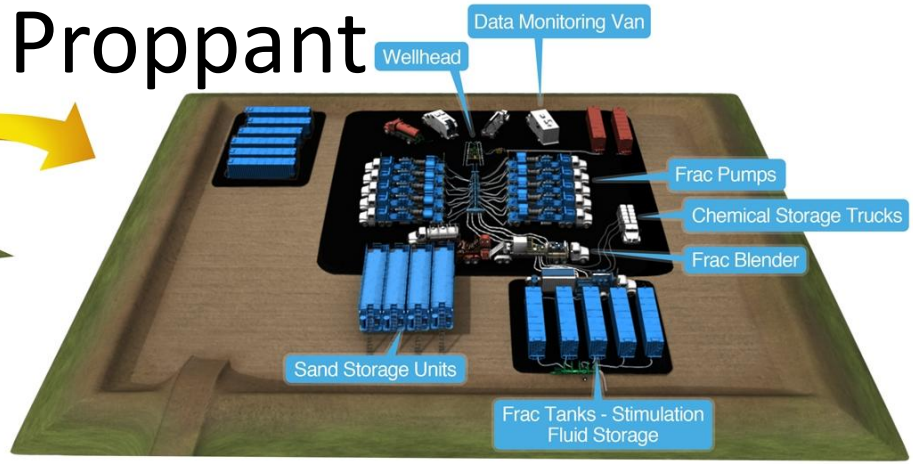

- Depth (1,500 ft, 1.5 sd)
  - Barnett 7,400 ft
  - Fayetteville 4,000 ft
  - Haynesville 11,400 ft
  - Marcellus 6,400 ft
- Target Reservoir Thickness
  - 200 100 ft

- Frac Job Material Volumetrics
  - Vary with operator, formation properties
  - volumetrics shown are for a “large” job
- Proppant
  - 5±2 *10^6 lbs (~30±12 *10^3 ft^3)
  - Mesh 100/40-70/20-40
- Frac Fluid
  - 120±20 *10^3 bbls (675±100 *10^3 ft^3)
  - “Slickwater” dominantly (part per million volume)
  - 3-11 chemical additives (all:1,000-6,000 ppmv)
    - Friction reducer, biocide, KCl subsitute , Fe chelator
    - Scale inhibitor, surfactant, non-emulsifier
    - Gel, crosslinker, breaker, corrosion inhibitor
    - All additives remain in Fluid except FR, Gel & XL
- Chesapeake Green Frac™

Chesapeake ENERGY

Fracture Stimulated Rock Volume

- Stimulated Rock Volume(SRV) geometry define by:
  - Microseismic
  - Frac material volumetrics
  - Frac modeling
  - Production Decline Analysis

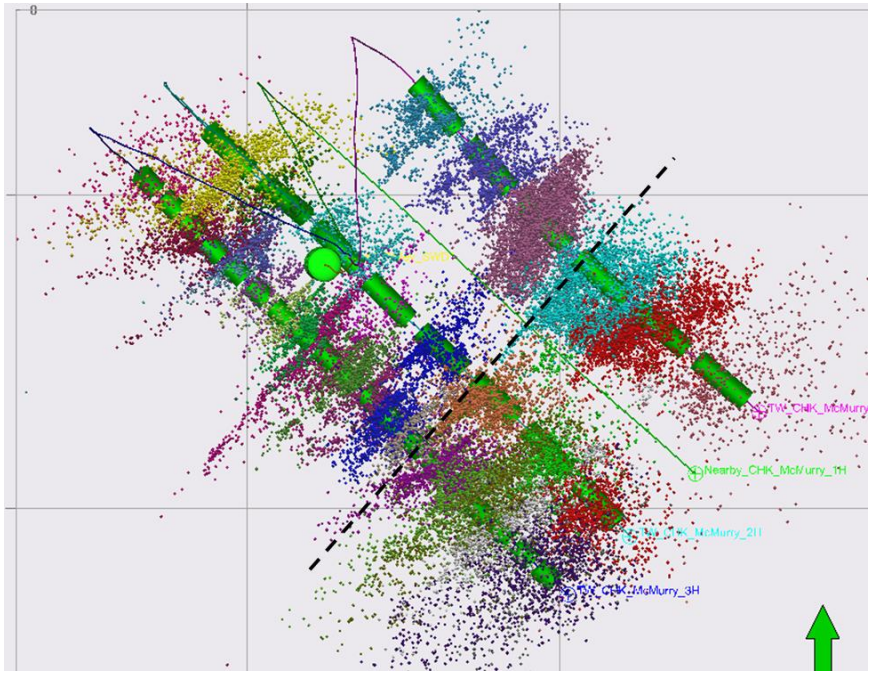

- **Parameters Involved**
  - Vertical stress profile
  - Regional and local principal stress anisotropy
  - Orientation of one/more natural fracture sets
  - Rock elastic properties
  - Fracture toughness
  - Frac fluid properties
  - Frac pump rates/pressures
  - Times between injection period
  - Proximity to frac barriers, nearby wells
  - Reservoir rock properties
    - Porosity
    - Permeability
    - Relative permeabilities
    - Initial water saturations
    - Capillary pressure properties
    - Pore throat size distribution

Chesapeake ENERGY

Fracture Architectures

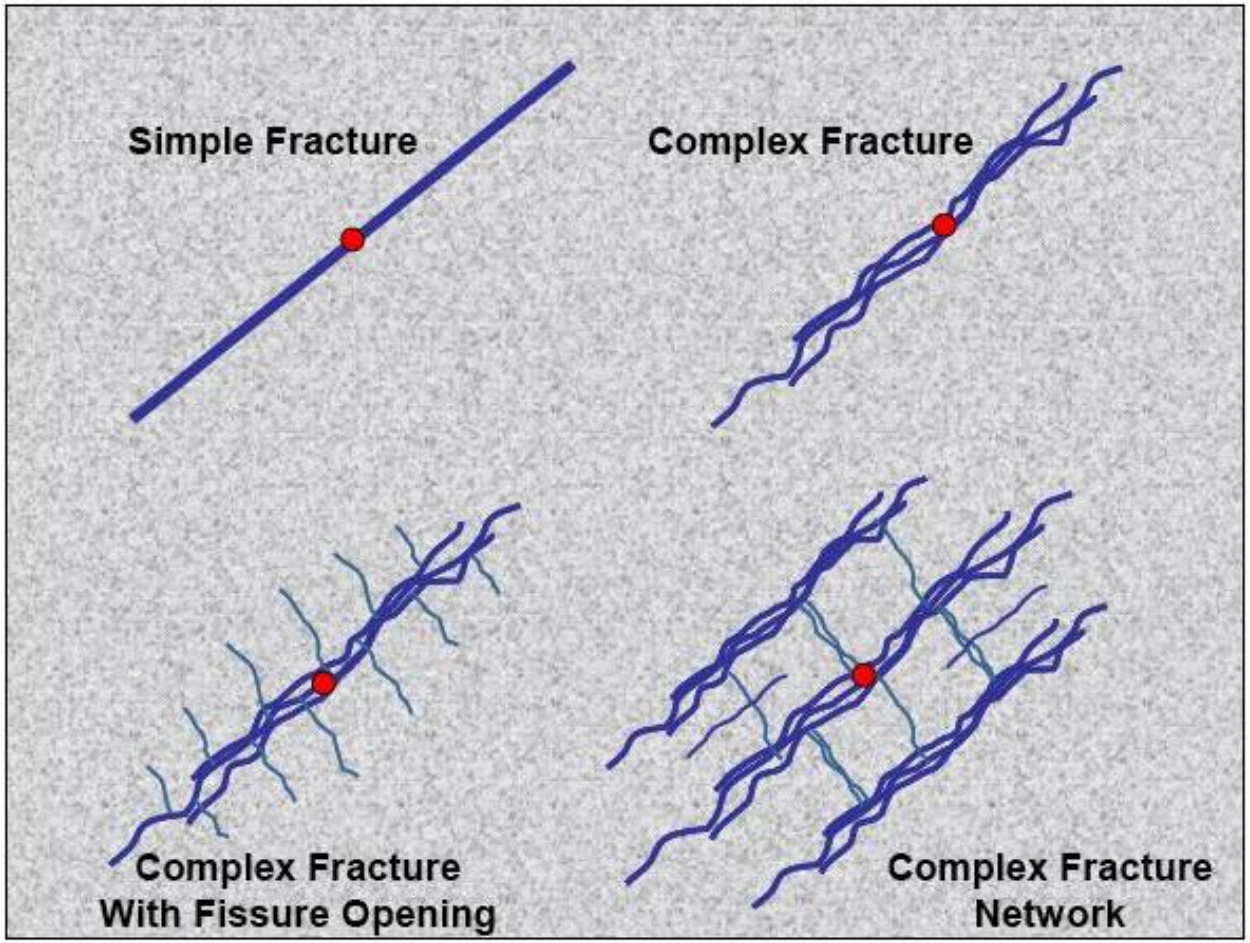

(modified from Fisher et al, 2002)

- Example of range of fracture architectures for a single initiation site
- These would occur at each perf cluster and so would be reproduced ~50-70 times along the wellbore

Chesapeake ENERGY

Production Decline Analysis and Flow Simulation

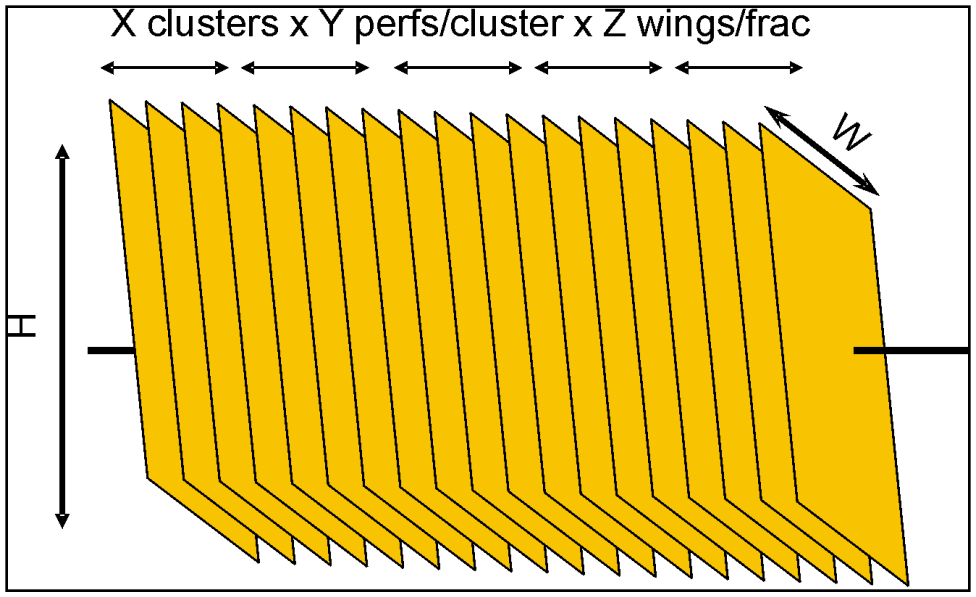

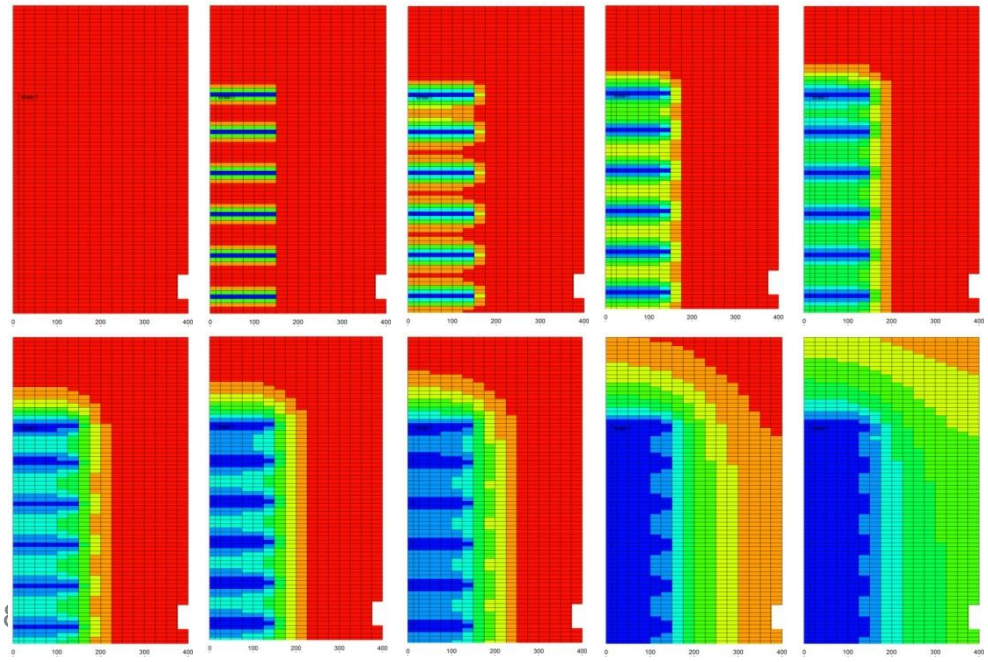

- Production Decline Analysis (PDA) & Numerical Flow Simulation Solve for $\mathbf{A}\sqrt{\boldsymbol{k}}$
  - Inputing core analysis $\boldsymbol{k}$ solve for **A**
  - **A** = 12 *10^6 ft^2
    - L = 4,700 ft
    - Fracs= 66 (70-ft spacing)
    - H=200 ft
    - W=400 ft
    - 2 sides of frac
- This surface area required for flow rates observed in wells
- 66 pairs of football fields
  - Flow into both faces

Simple flow simulation showing initial intrafrac flow followed by interwell flow

Chesapeake ENERGY

Created vs Effective: Proppant Distribution

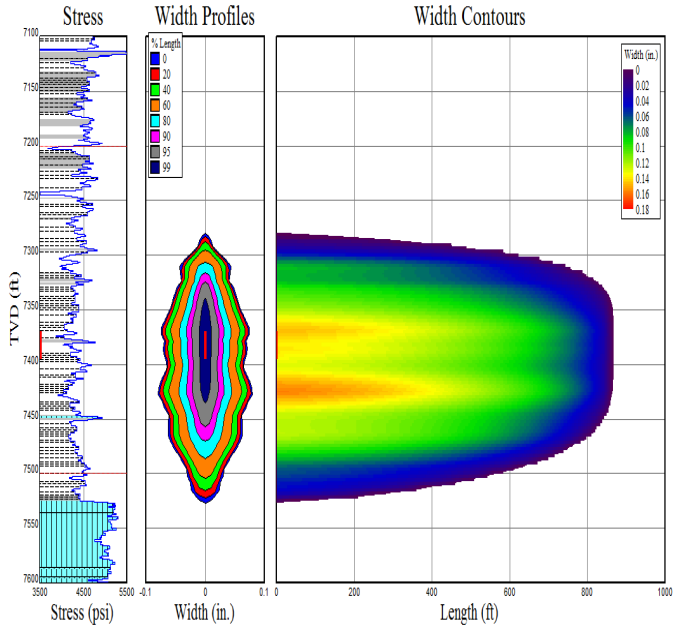

- Fracture Models
  - MFRAC/MSHALE (Meyer & Assoc.)
  - Volumetrics support 12 *10^6 ft^2 for effective propped frac surface area
  - Effective propped fracture 20%-50% total fracture
  - Models differ but surface area into which frac fluids are injected is approximately the same for all three architectures.

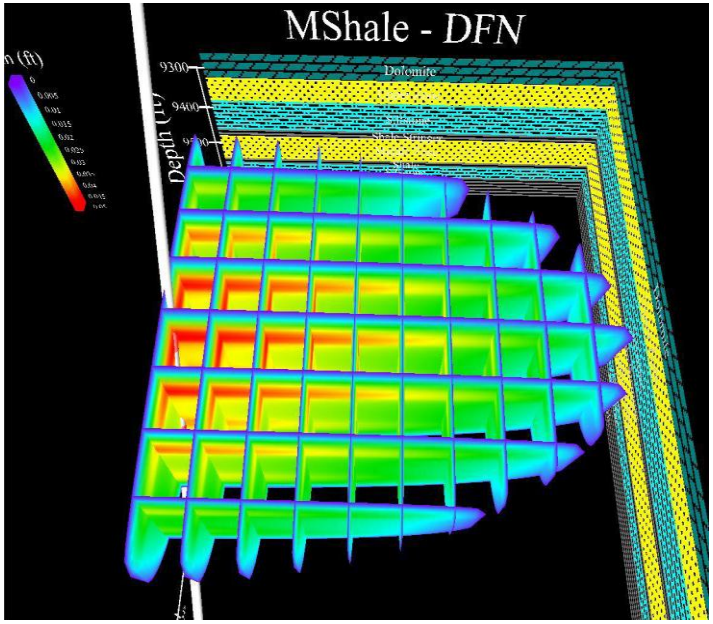

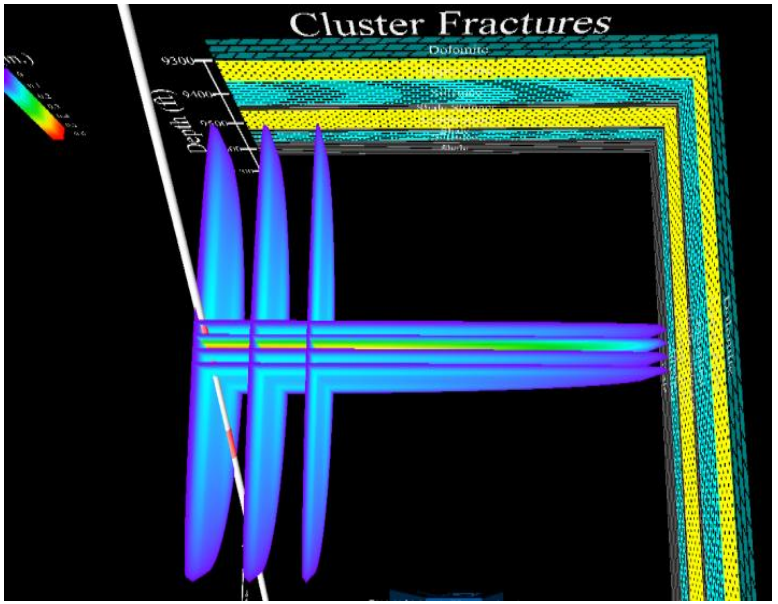

(DFN Figures courtesy of Meyer & Assocs. MSHALE)

Chesapeake ENERGY

Frac Surface Area – Induced Imbibition

- 12 *10^6 ft^2 Propped Effective
- Estimated Effective/Total
  - 20%-50% →
- Total Frac Surface
  - 24-60 *10^6 ft^2

- 120,000 bbls (670,000 ft^3) of frac fluid pumped
- Assuming uniformly injected
  - Variable = *f*(t)
- Porosity ϕ = 0.06
- Saturation depth ≈ 2 - 6 inches

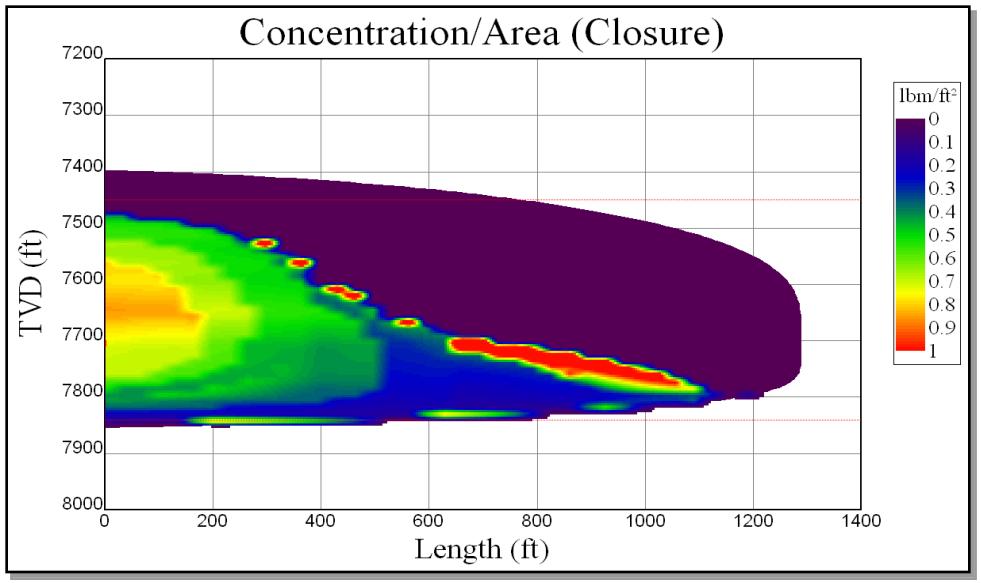

- Simple 1D Leakoff Model

$$q(t) = 4 \int_0^{A(t)} C/(t-t_o)^{0.5}\, dA$$

q(*t*) = fluid loss rate at time *t*
A(*t*) = fracture area of one face
C = total leakoff coefficient
t_o = time of fracture area creation

Chesapeake ENERGY

Porosity & Kerogen Properties

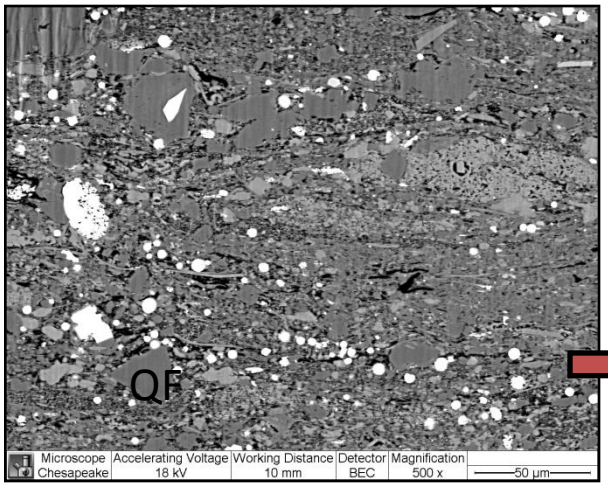

Laminated argillaceous to calcareous mudstone to silty mudstone

$$\phi_{total} = \phi_{intergranular} + \phi_{intrakerogen}$$

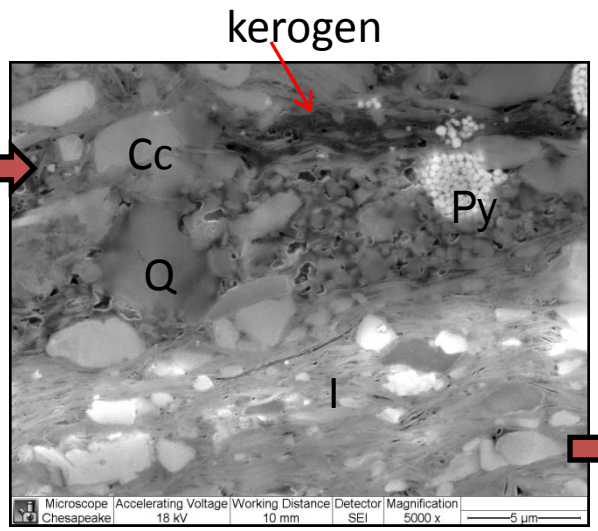

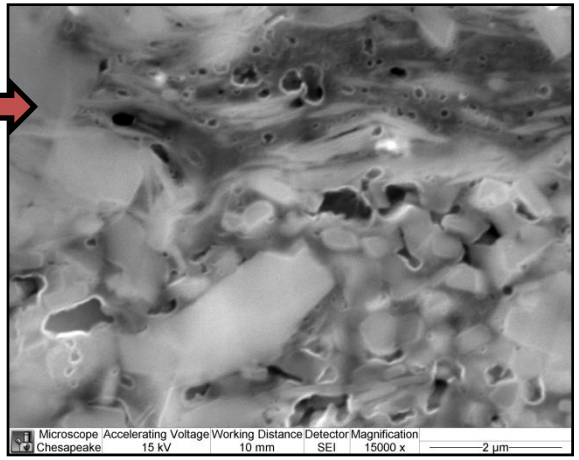

- Porosities vary by play and within reservoir intervals
- 3-10%
- General value 6%

Chesapeake ENERGY

Pore Throat Diameter vs. Permeability

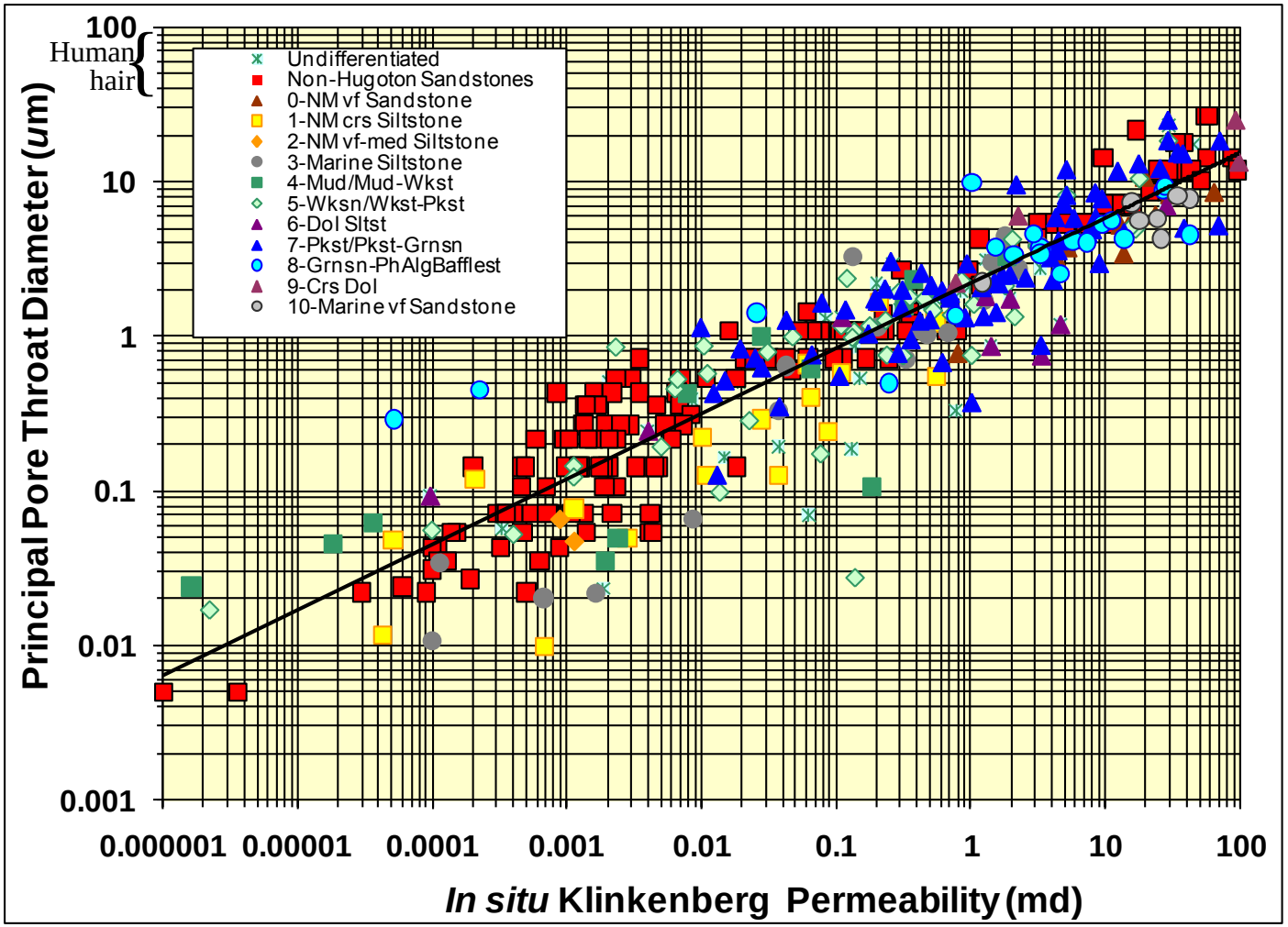

(after Byrnes, 1997, 2005)

- Permeability for all lithology rocks is principally controlled by pore throat size (the "chokes" in the flow path)
- For Mudstones of present commercial interest (50 nD < k < 2,000 nD) corresponding D_{pt} are 0.01 μm < D_{pt} < 0.2 μm
- "Typical" pore throat size distribution ranges from 10-20X so for 500 nD rock 0.004 μm < D_t < 0.09 μm

Chesapeake ENERGY

Threshold Entry Pressures

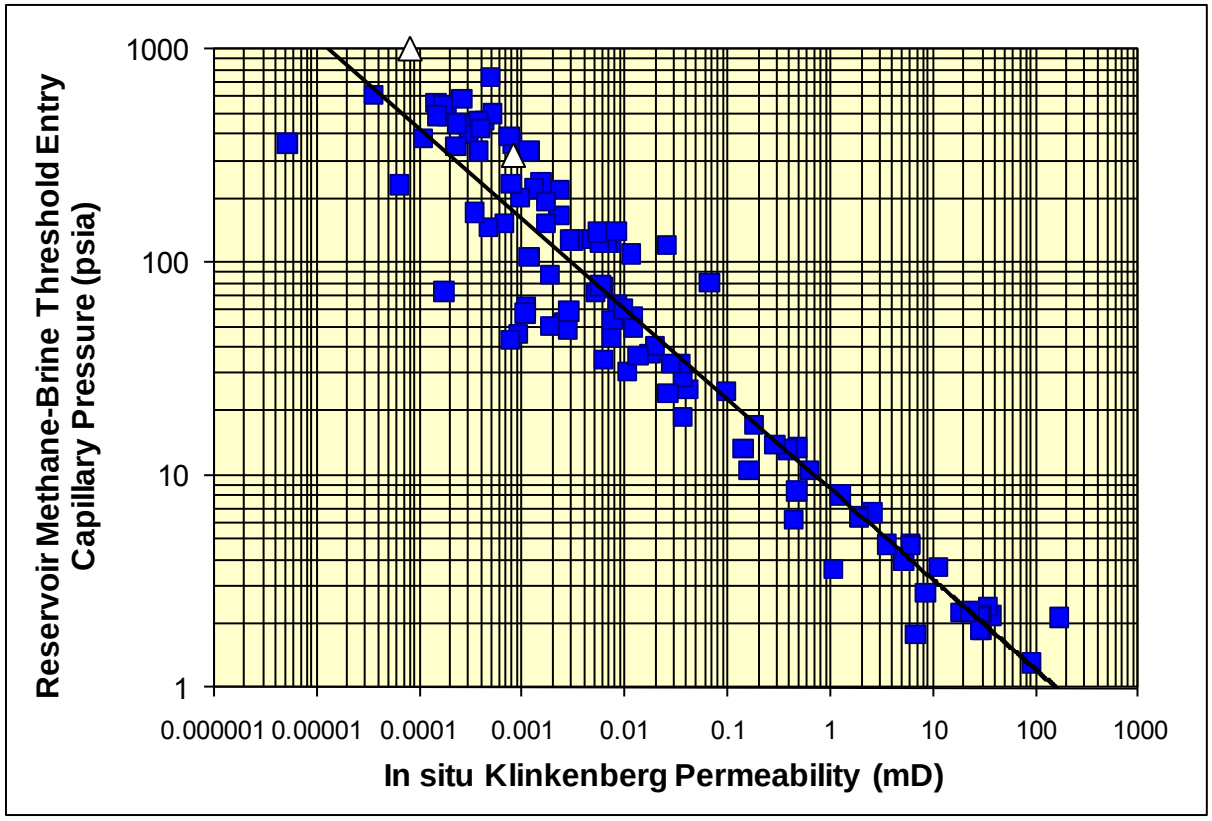

(modified from Byrnes 2009)

- Threshold entry capillary pressures (P_{te}) for lithic sandstones (blue squares) and representative gas shales (open triangles).
- P_{te} were measured using air-Hg and converted to equivalent reservoir CH_4-Brine pressures.
- Data for shale show continuity with trend for sandstones and siltstones. Relationship can be expressed:
- $P_{te} = 8.6\ k_i^{-0.424}$

Chesapeake ENERGY

Gas Shale vs Low-k Sandstone Capillary Pressure

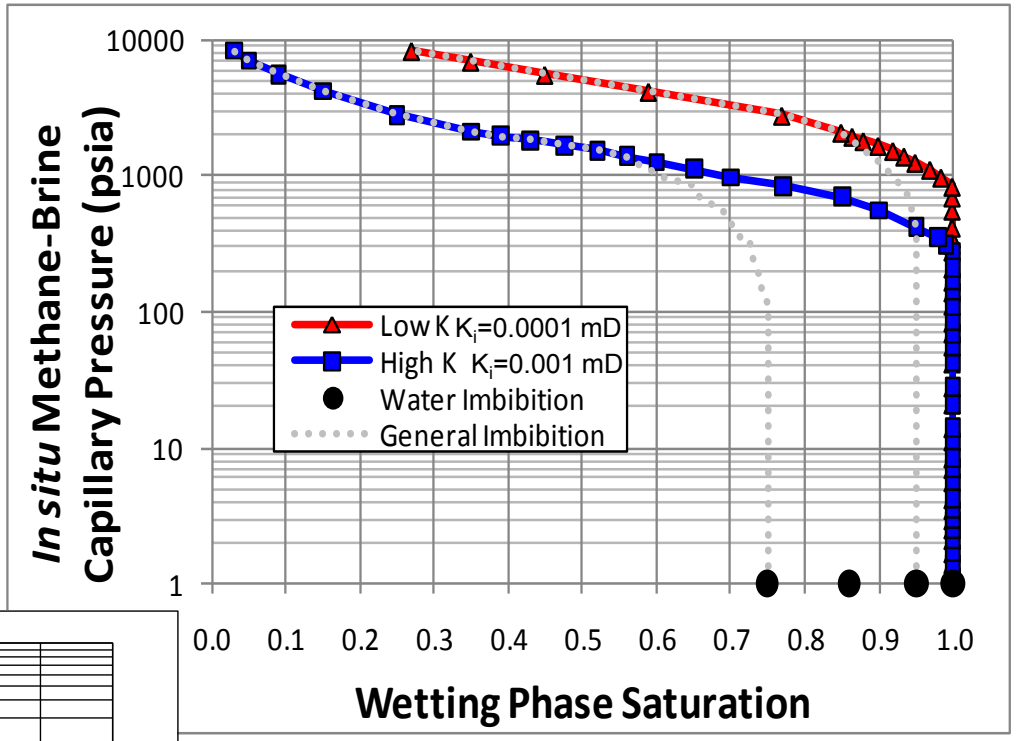

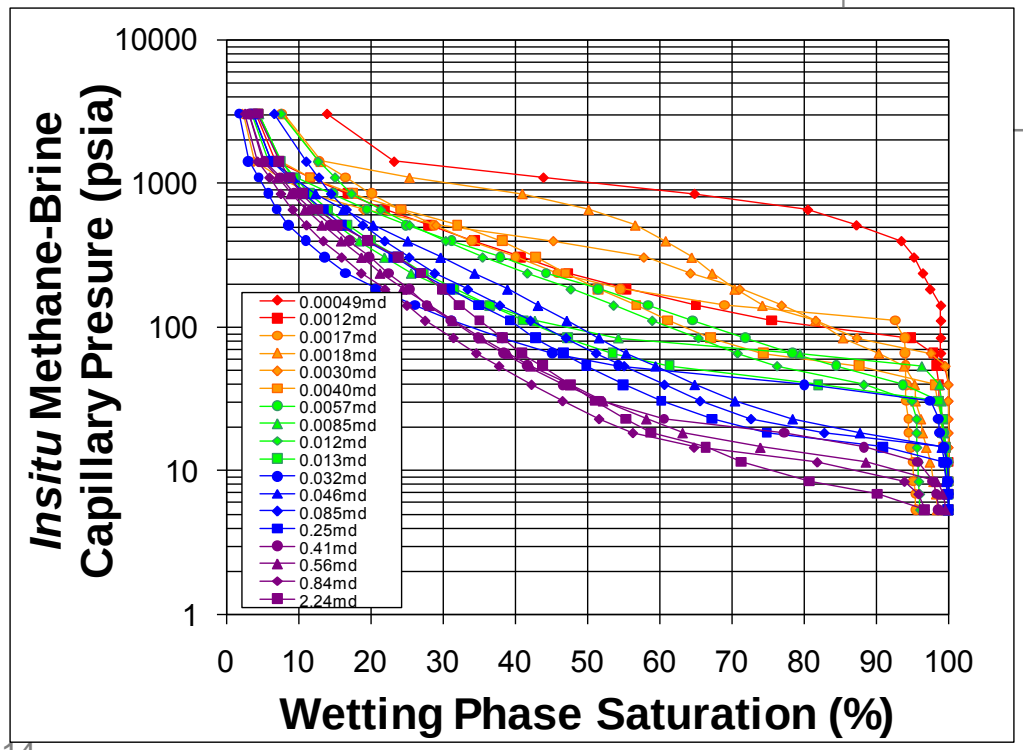

- Theshold entry pressure (P_{te}) increase with decreasing permeability
- Gas shales exhibit higher threshold entry pressures consistent with texture and permeability
- Capillary pressure distribution is approximately 10X-20X from P_{te}

Chesapeake ENERGY

Shale Capillary Pressure Properties

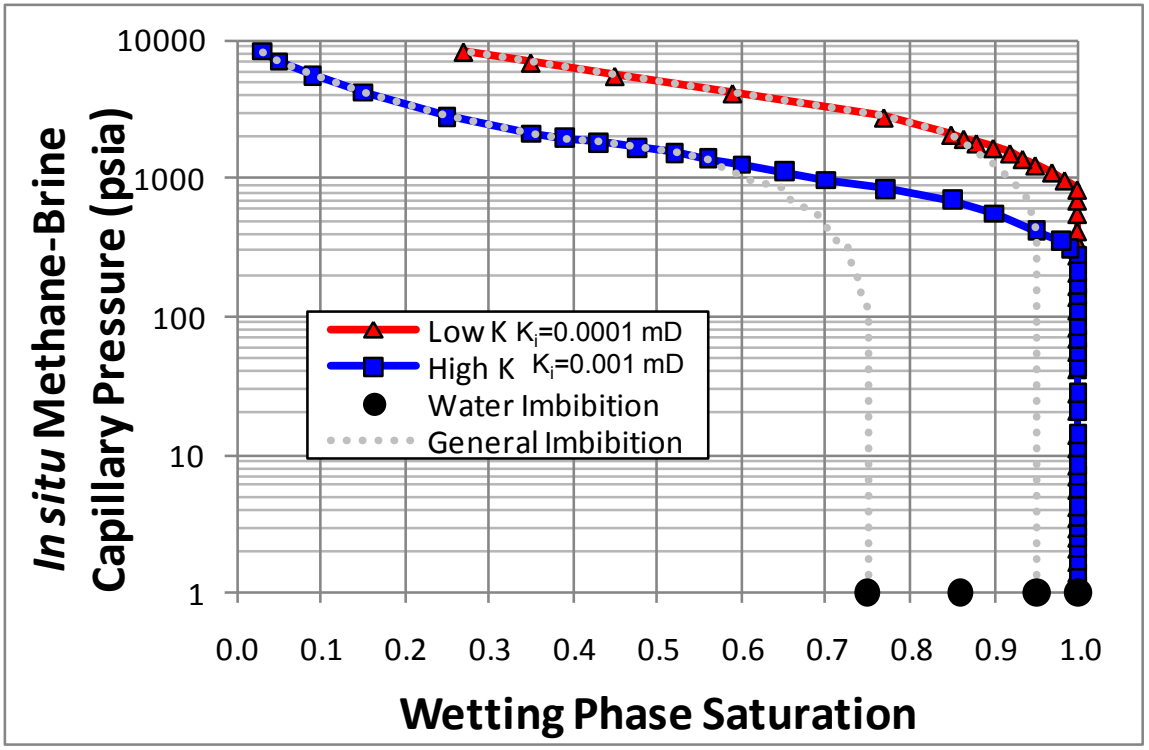

- 0.002 mD > ki > 0.00005 mD
- 120 psi < P_{te} < 600 psi
- Pc increases with decreasing water saturation.
- Capillary pressures (Pc) required to achieve or maintain the brine saturations in the present-day reservoirs (0.2 < Sw < 0.5) do not exist in all reservoirs today.

- Capillary pressure properties of present day reservoir do not necessarily represent conditions at time of desaturation
  - reservoir exhibited better properties at time of gas generation allowing desaturation at lower Pc
- Present Reservoir
  - Nonequilibrium and undersaturated
  - Equilibrium but has mixed or intermediate wettability.
- Natural imbibition of water to Sw>0.75 for gas shale cores tested (black circles)
  - requires reservoir is sufficiently water wet to imbibe water with change in capillary pressure conditions
  - Imbibition curves, based on low-k sandstone, show general path of imbibition Pc curve

Chesapeake ENERGY

Shale Capillary Pressure Properties

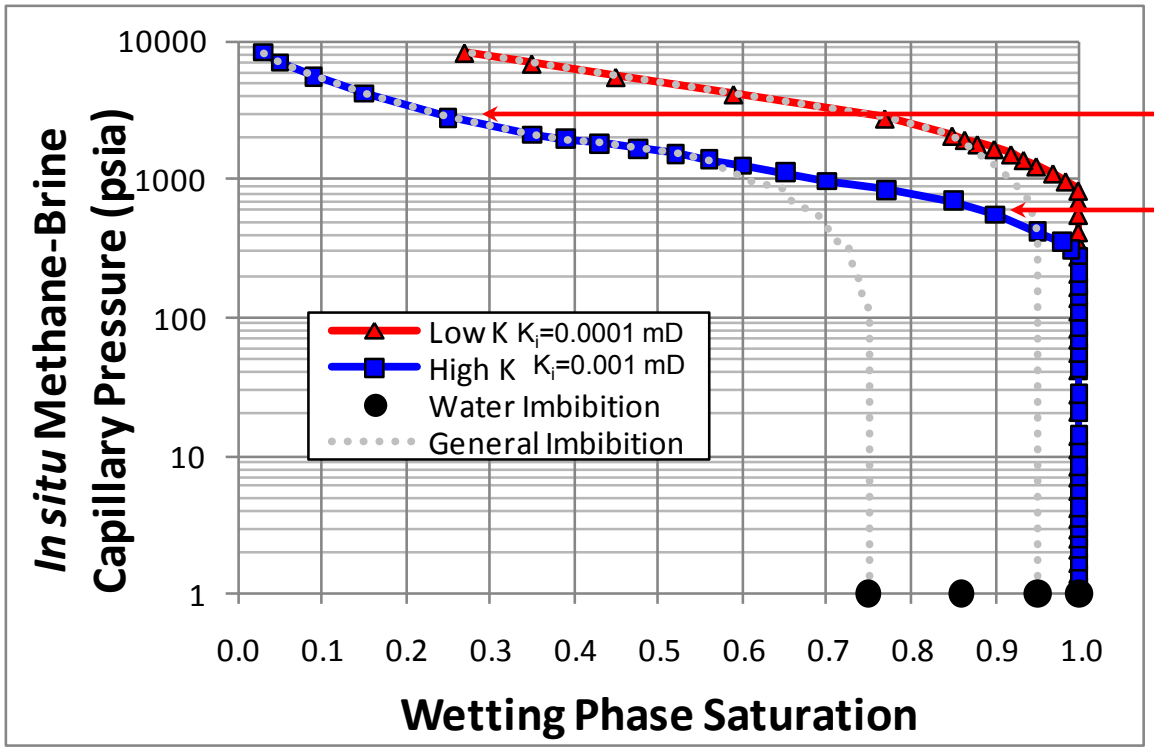

- After frac for 2-6 inches into the formation from the frac face Sw is~100%
- Reservoir Sw ~30%
- Capillary pressure difference between these two Sw states is 100's-1,000's of psi

- Capillary pressure difference between the reservoir and the frac face causes frac fluids to move to reservoir – natural imbibition
- **System is driven by Pc to uniform saturation state**
  - **to achieve uniform Sw the high Sw in frac-face region must imbibe**
- Rate of movement; $q(t) = f(k_{ew}, Sw, Pc, \phi)$

Chesapeake ENERGY

Fate of Frac Fluids

- Initial production produces 30 ±10% of frac fluid
- Remaining 70±10% of fluid leaks off into formation

- If well is shut in natural imbibition works unhindered

- If well is placed on production immediately then viscous forces and low near-frac face pressures slow or halt natural imbibition
- As near-frac face region gas pressures drop the lower Pc condition “locks” in the Sw state and fluids are held in place

- With complete pressure depletion of the well the low Pc condition of the reservoir traps all fluid in place
- In pressure depleted state the reservoir is undersaturated and over geologic time acts to imbibe water

Conclusions

- Hydraulic fracture modeling and fracture surface area calculations determined from pressure decay analysis and reservoir numerical flow simulation support. estimates of created hydraulic fracture surface areas of 24-60 $*10^6$ sq ft.
- 30±10% of the frac fluids are recovered.
- 70±10% leaks off into the fracture face resulting in elevated frac fluid saturations within ~2 – 6 inches of the frac face.
- High frac-face Sw is not in equilibrium and capillary forces act to imbibe the fluid into the reservoir away from the frac face
- Frac fluids imbibed into the formation are effectively locked in place by capillary pressure forces of hundreds to thousands of pounds per square inch (psi) both during the life of the well production and for geologic periods of time after reservoir depletion.
- Further research is needed and is ongoing as to the exact shape of the imbibition capillary pressure curves and imbibition water relative permeability curves to fully quantify the imbibition process and timing.

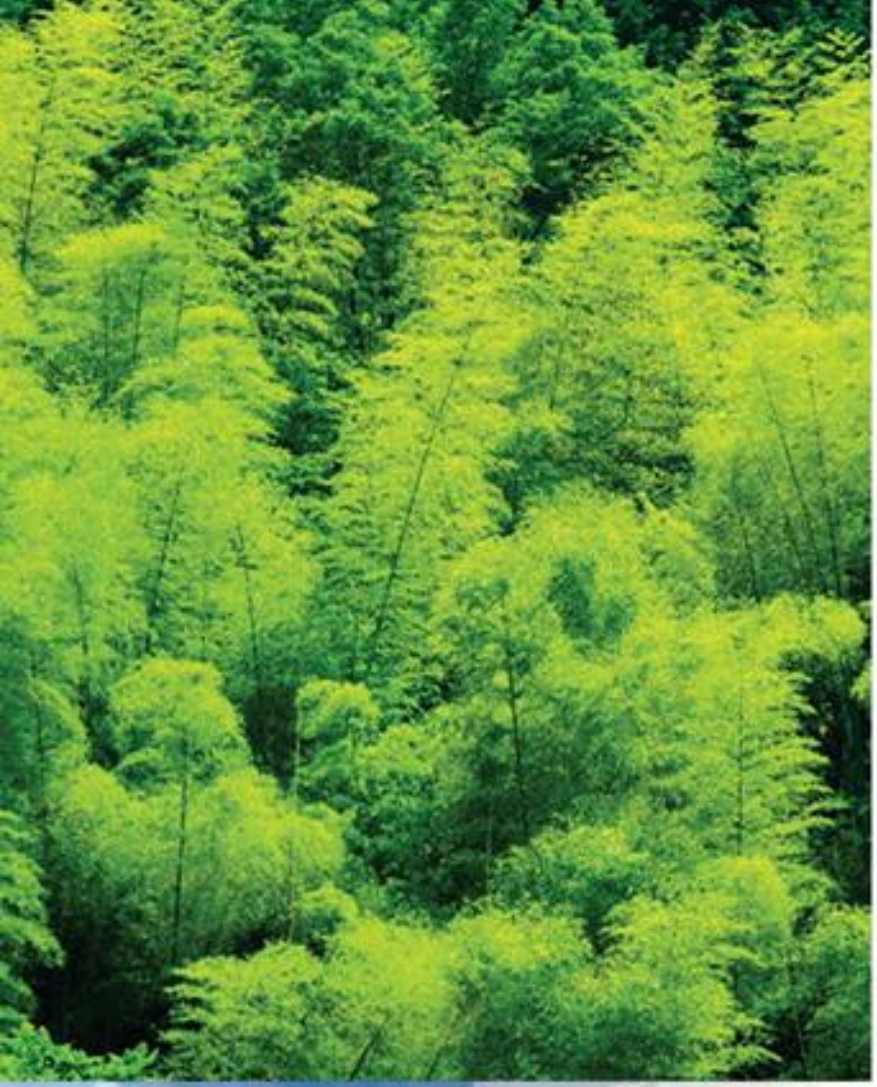

"Thank You – Questions?"

Alan P. Byrnes
Chief Petrophysicst

Role of Induced and Natural Imbibition in Frac Fluid Transport and Fate in Gas Shales

Alan P. Byrnes
Chesapeake Energy Corporation

The statements made during the workshop do not represent the views or opinions of EPA. The claims made by participants have not been verified or endorsed by EPA.

Abstract

Hydraulic fracture modeling and fracture surface area calculations determined from production data analysis and reservoir numerical flow simulation support estimates of created hydraulic fracture (frac) surface areas of 24-60 MM sq ft for representative hydraulic fracture treatment designs. Approximately 30±10% of the frac fluids are recovered and the remaining 70±10% leaks off into the fracture face resulting in elevated frac fluid saturations within 2 – 6 inches of the fracture face. Although natural imbibitions capillary forces can generally be ignored in conventional reservoirs, in gas shales these forces can range from 200-2,000 psi. Drainage and imbibition capillary pressure analysis indicate that the elevated near frac-face saturations are not in equilibrium and capillary forces act to naturally imbibe the fluid back into the reservoir away from the frac face. This process occurs over weeks to months and can be slowed or halted by gas pressure decrease associated with well production. The frac fluids imbibed into the formation are effectively locked in place with the native brine by capillary forces both during the life of the well production and for geologic periods of time after reservoir depletion.

Introduction

Gas shale reservoirs characteristically exhibit low porosity (ϕ = 3-10%), low *in situ* specific permeability (k_i = 50–2,000 nD), low water saturation (Sw = 10-50%) and thickness of H = 50-400 ft over large regions. To achieve economic gas production rates for these matrix properties, flow to the wellbore is enhanced using multi-stage hydraulic fracture stimulation. Present optimum well designs vary among operators and with reservoir properties but can be broadly characterized as comprising horizontal wells with 4,500±1,000 ft of lateral length and with up to 60±20 fracture clusters along the wellbore. In a "large" hydraulic fracture stimulation (frac) as much as 5±2 million pounds of proppant may be used, transported by 120,000±20,000 bbls of frac fluid, where 30±10% of the frac fluid is typically recovered during production. Understanding the transport and fate of these frac fluids is important for environmental and optimum well stimulation design reasons.

Frac fluid flows into and out of the rock formation through the frac face can be characterized as comprising three flow periods: 1) an induced imbibition period during and immediately following the frac treatment and dominated by pressure-induced leakoff, 2) a natural imbibition period when the well is shut-in following stimulation and capillary forces influence frac fluid redistribution, and 3) flow out of the formation resulting from pressure drawdown in the

fracture and when capillary and viscous forces are potentially competing. Numerous studies have explored hydraulic fracture modeling, which implicitly involves transport or flow of frac fluids both in induced and natural fractures and into the formation through the created fracture face. Published studies have extensively explored issues involving leakoff of fluids during fracture creation and after pumping during fluid pressure decay. Foundational work by Nolte (e.g., 1979, 1986, 1993) explored the relationships describing fluid leakoff associated with initial spurt loss and subsequent filter-cake limited pressure-dependent leakoff. Additional work has explored and summarized previous work on such issues as fluid loss in natural fractures (Warpinski, 1990), effective fracture length (Barree et al, 2003; Cipolla et al, 2008), leakoff and permeability (Meyerhofer and Economides, 1997), and fracture modeling (Barree, 1983; Meyer et al , 1990; Cipolla et al, 2011).

Fluid flow is influenced by two forces; 1) viscous force associated with induced pressure differences resulting from pumping or well production, and 2) capillary force associated with interfacial tension among fluids and the rock pore surfaces. Capillary forces can generally be ignored in reservoirs with k > 0.01 mD because reservoir methane-brine capillary forces are generally only 1-100 psi and these forces are small compared to viscous forces associated with flowing pressure drops. In contrast, very low permeability reservoir (0.000001 mD < k < 0.001 mD) threshold entry methane-brine capillary pressures ($P_{te} = Pc_{,Sw=1}$) range from approximately P_{te} = 200-2,000 psi and increase with decreasing water saturation. At these levels the influence of capillary pressure on fluid movement and distribution cannot be ignored and can play a significant role in the transport and fate of frac fluids. The influence of high water saturations near the frac face were investigated by Holditch (1979) and more recently by Cheng (2010). Cheng's analysis illustrated the significant role that natural imbibition can play in fluid distribution but did not fully explore properties at high capillary pressures.

This brief abstract will utilize the above work and laboratory data to broadly analyze the transport and fate of frac fluids in representative hydraulic fractures and illustrate that the low fluid recoveries from frac treatments are consistent with the fracture and rock properties and that once frac fluids are imbibed into the reservoir capillary forces act to imbibe them away from the frac face and hold them in place with capillary pressure forces of hundreds to thousands of pounds per square inch (psi). The initial high water saturations result in near-frac face blockage and reduced gas flow rates but natural imbibition results in a decrease in Sw over time and "cleanup" of the frac face and consequent increase in gas flow rates. The cleanup period is influenced by such variables as the volume of water introduced, the permeability and effective water permeability of the reservoir, whether the well is flowing or shut-in, the near-frac face pressure, and the specific capillary pressure properties of the reservoir rocks and can occur over periods of weeks to months.

Frac Fluid Composition

Many variables are involved in fracture fluid chemistry design. Prior to pumping any fluid systems, fluid-rock core measurements are used to determine the minimum fluid additives necessary in each play to prevent formation damage from drilling or fracture fluids. The majority of the shale plays in North America are treated with a large percentage of "slickwater."

Slickwater is predominantly fresh water with four to eleven chemical additives at a combined concentration of 1,000-6,000 parts per million by volume (ppmv) or 0.1-0.6 percent by volume of the liquid pumped. Light gels are often used at the end of a stage to transport higher sand concentrations. Chesapeake Energy's Green Frac™ program was initiated in 2009 to eliminate additives not critical to successful completion and to replace necessary additives with more environmentally benign chemicals.

Hydraulic Fracture Architecture and Induced Frac Fluid Imbibition

Numerous models exist for hydraulic fracture architectures and can broadly be classified as ranging from simple planar fractures to complex fracture networks (Figure 15). The nature of the fracture architecture that develops at any given location is a function of numerous variables including but not limited to: magnitude of direction of horizontal stress field; vertical stress profile; regional and local principal stress anisotropy; presence and orientation of one or more natural fracture sets; rock elastic properties; fracture toughness; vertical and lateral heterogeneity of rock properties; frac fluid properties; frac pump rates, pressures, and times between injection period; proximity to frac barriers, nearby wells, and adjacent well histories; and reservoir rock properties including porosity, permeability, relative permeabilities, initial water saturations, capillary pressure properties, pore throat size distribution, etc.

Based on the influence and interaction of these variables, fracture architecture will vary among different shale plays, within a shale play, along a given horizontal well, and potentially even within a given frac stage. Microseismic data can be interpreted to support the predominance of a given frac architecture within given areas. For the range of frac architectures that can occur, frac modeling indicates that the proppant is deposited in a region representing only 20-50% of the total fracture system (Figure 16).

Figure 15. Example of range of fracture architectures for a single initiation site. (modified from Fisher et al, 2002).

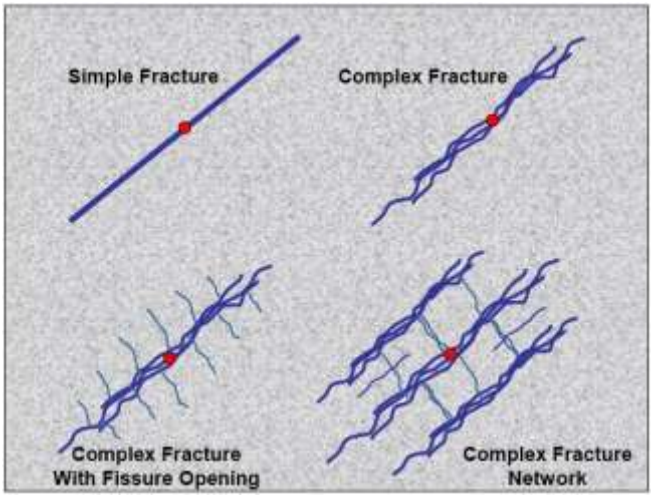

Total effective surface area can be estimated using frac modeling, pressure transient analysis (PTA), production data analysis (PDA), and numerical flow simulation (NFS). These methods provide non-unique solutions that model observed pressure and flow behavior through time. Production decline analysis provides a solution for A√k (Area * $k^{0.5}$). Knowing *in situ* reservoir effective gas matrix permeability from core analysis, it is possible to define the total effective fracture surface area from the early production and pressure data that is characterized by transient unsteady-state flow (e.g., Miller et al, 2010). These methods indicate that "large" hydraulic fracture stimulation treatments utilizing approximately 120,000 bbls of fluid and 5 million pounds of proppant create effective fractures with surface

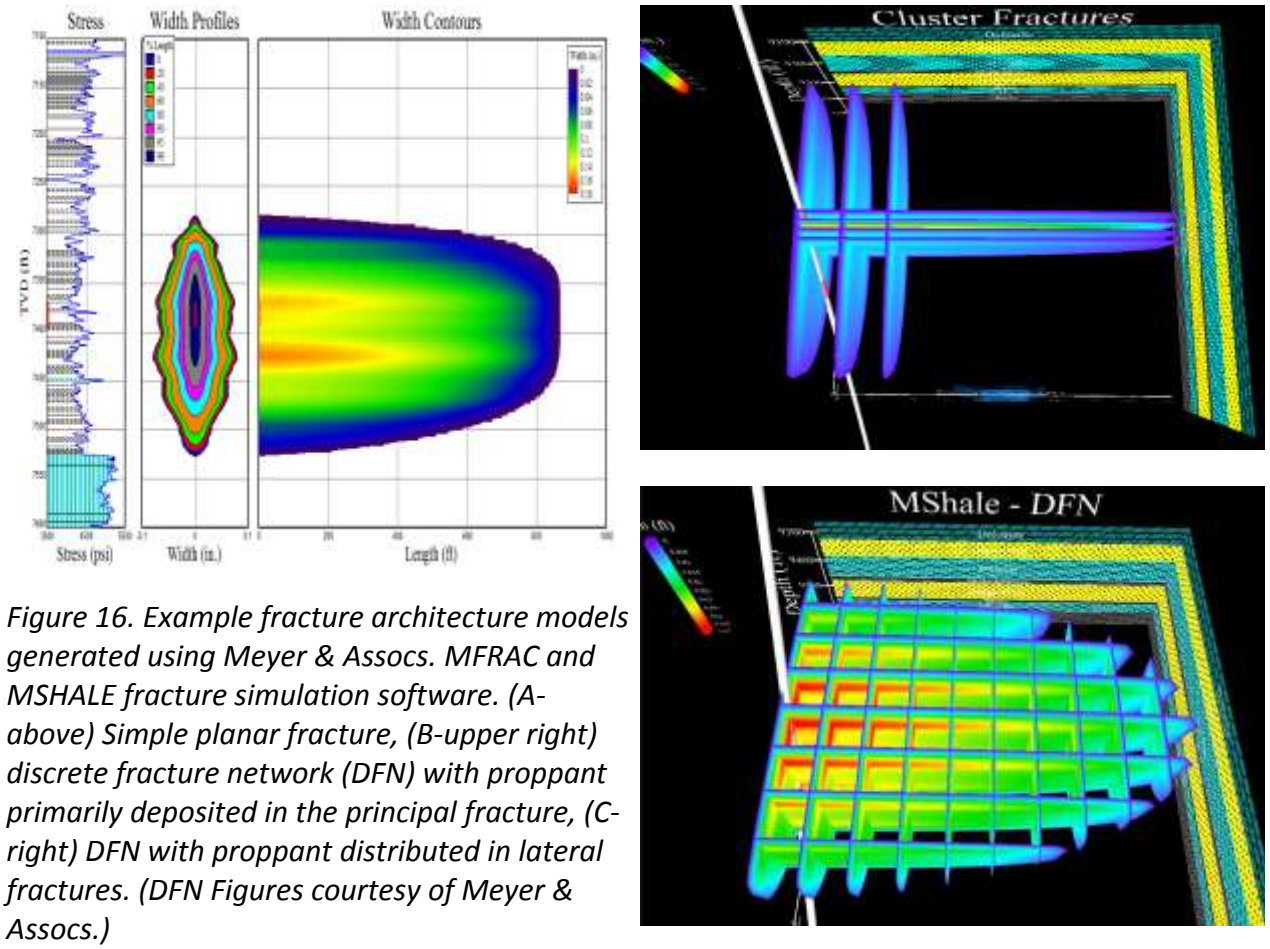

Figure 16. Example fracture architecture models generated using Meyer & Assocs. MFRAC and MSHALE fracture simulation software. (A-above) Simple planar fracture, (B-upper right) discrete fracture network (DFN) with proppant primarily deposited in the principal fracture, (C-right) DFN with proppant distributed in lateral fractures. (DFN Figures courtesy of Meyer & Assocs.)

areas of approximately 12 MM sq ft (12 * 10^6 sq ft). Assuming the effective fracture surface area is 20-50% of the total, the total fracture surface area created is approximately 24-60 MM sq ft. This range in values is consistent with the total surface area estimated for either a simple planar fracture, compared to the high proppant concentration area (Figure 16), or for a central principal fracture or fracture set surrounded by unpropped or stranded lateral complex fractures (Figure 16). Generally, limited by material balance constraints and the PDA-defined surface area, a simple planar fracture potentially exhibits greater height or more effective half-length than the DFN architectures.

Although the three fracture models shown in Figure 16 differ in architecture, PDA and numerical flow simulation show that for the same effective fracture surface area, the initial transient unsteady-state flow is identical and that differences in production do not occur until inter-frac interference begins. This issue is highly relevant to optimum gas well production. However, for frac fluid transport, the surface area created by the fracing process, and the surface area into which frac fluids are injected, is approximately or can be exactly the same for all three architectures. Differences in fracture architecture do not necessarily significantly change the total surface area into which frac fluids flow.

Fracture modeling shown in Figure 16 provides the basis for defining the distribution of frac fluid in the near-frac face region for all fractures shown. Volumes of frac fluid induced to imbibe into the formation are defined by various forms of the leakoff equation that describes initial spurt loss (i.e., the initial loss of fluid before a filter cake is formed) followed by filter-cake controlled leakoff. In it simplest 1D form (Carter, 1957), the total fluid leakoff rate can be characterized by:

$$q(t) = 4 \int_0^{A(t)} C/(t-t_o)^{0.5}\, dA \qquad [1]$$

where q(t) is the fluid loss rate at time t, A(t) is the fracture area of one face, C is the total leakoff coefficient (including the initial spurt loss coefficient), t_o is the time of fracture area creation.

Although injected volumes are greater near the fracture initiation location due to longer times of injection, and are greater in higher permeability rocks, the volume of frac fluid injected at any given point on the frac face can be very approximately estimated assuming the total volume injected is uniformly distributed over the frac face surface area. For 120,000 bbls (670,000 ft^3) of frac fluid pumped, assuming this is uniformly injected into 24-60 MM sq ft, then the depth of penetration (D_{ffp}) of a 100% saturated interval, in a rock with ϕ = 0.06 is $D_{ffp} \tilde{}$ 2-6 inches.

Typically, following a large fracture stimulation treatment a well will be produced to recover as much frac fluid as possible and then the well will be shut in for different time periods depending on operator practices, surface facilities construction or hookup, or pipeline scheduling. This initial production removes most of the frac fluid in the effective propped fracture and the shut-in period initiates the time of natural imbibition. Whether the well is shut-in or begins production, following induced imbibition the frac fluids in the near-frac region are influenced by natural imbibition resulting from capillary pressure forces.

Natural Imbibition

Elevated frac water saturations in the near frac-face region are not in capillary pressure equilibrium. Air-mercury capillary pressure curves (converted to equivalent reservoir-condition methane brine pressures), generally representing the bounding range of those observed for gas shales with specific *in situ* Klinkenberg permeability ranging between 0.0002 mD > ki > 0.00005 mD, illustrate that threshold entry methane-brine capillary pressures ($P_{te} = Pc,_{Sw=1}$) range from approximately 2,000 psi > P_{te} > 250 psi and increase with decreasing water saturation (Figure 17). These threshold entry pressures are consistent with threshold entry pressure-permeability relationships exhibited by lithic low-permeability sandstones and siltstones (Figure 18). Because the drainage curves in Figure 17 were measured using air-mercury, they represent drainage conditions where all pore surfaces are wetted by the wetting phase. The capillary pressures required to achieve or maintain the brine saturations in the present-day reservoirs (0.2 < Sw < 0.5) do not exist in the reservoirs today. It can be hypothesized that the low reservoir water saturations were created by displacement of connate brine from the rock pore space during oil

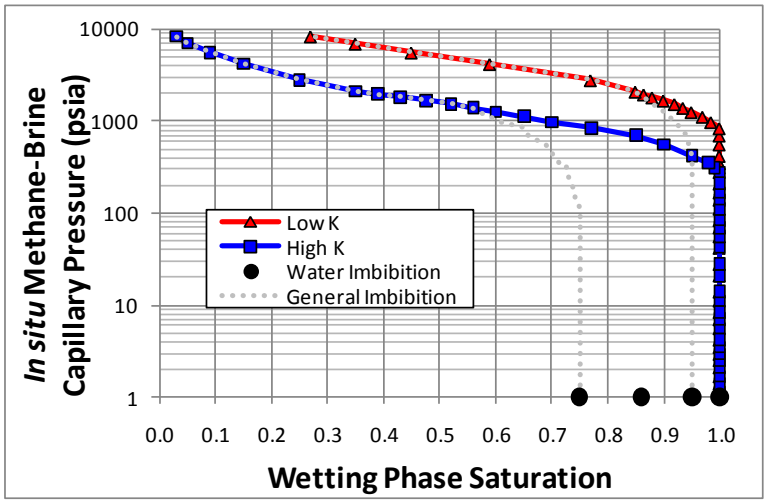

Figure 17. General representative drainage capillary pressure curves for gas shales of low k (0.00005 mD; red triangles) and high k (0.002 mD; blue squares) measured using air-Hg and converted to equivalent reservoir CH4-Brine pressures. Also shown are measured water saturations for natural imbibition of core from as-received saturation (black circles). Grey dashed curves represent generalized imbibition curves modeled from low-k sandstones.

or gas generation when the formation rock was more porous, permeable and exhibited a lower capillary pressure. Additionally, the development of intra-kerogen porosity during catagenesis, which did not require displacement of brine, increased the total porosity and consequently decreased brine saturation because the brine saturation is referenced to the total pore volume. Water adsorption measurements indicate that kerogen surfaces exhibit mixed wettability and portions are both hydrophobic and hydrophilic. Under these conditions, the capillary pressure curves shown represent an end-member condition and methane-brine capillary pressure curves at reservoir conditions can exhibit lower slopes but still require similar threshold entry pressures because these are determined by the interparticle pore system of the water-wet mineral grains. An alternate model for capillary pressure-saturation conditions is that the reservoirs are presently undersaturated and are not in capillary equilibrium. For this nonequilibium condition, the reservoir would presently be working to naturally imbibe water from surrounding formations but may be limited by availability of water, extremely low water relative permeability, and potential partial influence of a mixed wettability condition.

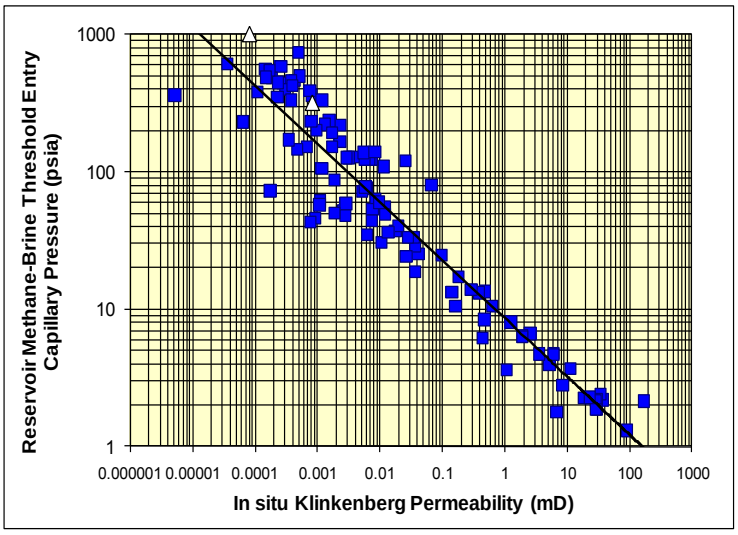

Figure 18. Threshold entry capillary pressures (P_{te}) versus specific in situ Klinkenberg permeability for lithic sandstones (blue squares) and representative gas shales (open triangles). P_{te} were measured using air-Hg and converted to equivalent reservoir CH_4- Brine pressures. Data for shale show continuity with trend for sandstones and siltstones. Relationship can be expressed: $P_{te} = 12.25\ k_i^{-0.424}$.

The wettability and imbibitions properties of gas shales can be tested by performing imbibition capillary pressure measurements on core in as-received condition. Typically wettability is measured using the Amott or USBM methods but these methods are experimentally difficult to perform on gas shales due to their low permeability and high capillary pressures. A simple limiting condition test is to perform a natural imbibition test which represents the condition of brine imbibition at low gas-brine capillary pressure and the resulting equilibrium brine saturations. For this test, if kerogen surfaces are hydrophobic then brine will only be imbibed into the water-wet portions of the mineral-lined pore pace and a trapped residual gas saturation, representing the gas in the kerogen pores, will result. If the kerogen pore surface is sufficiently hydrophilic then water is imbibed into the complete pore space and residual trapped gas saturations are low. The imbibition data shown in Figure 17 for the condition of 1 psi capillary pressure indicate that gas shales are capable of naturally imbibing water leaving very low residual gas saturations.

Research on the exact imbibition capillary pressure curve shape is on-going but curve shapes characteristic of low-permeability sandstones and siltstones (Byrnes and Cluff, 2009) are likely to be representative (Figure 17). These curves indicate that imbibition capillary pressure forces between the elevated water saturations near the frac face and the lower water saturations in the reservoir produce a capillary pressure drive mechanism of hundreds to thousands of psi. This force acts to naturally imbibe the frac water away from the frac face and into the formation where it is held in place by those same forces.

If the well is produced before the high water saturations are reduced near the frac face then the elevated near frac-face water saturations can be stabilized by the lower capillary pressures that can result from gas pressure depletion. When a well is fully pressure depleted it can be projected that the reservoir would naturally imbibe water from surrounding intervals. The time period over which this occurs would be a function of many variables including the formation effective water permeability, surrounding formation effective water permeabilities and capillary pressures in the formation and in the surrounding formations.

Discussion

Hydraulic fracture modeling and fracture surface area calculations determined from pressure decay analysis and reservoir numerical flow simulation support estimates of created hydraulic fracture surface areas of 24-60 MM sq ft. Approximately 30$\pm$10% of the frac fluids are recovered and the remaining 70$\pm$10% leaks off into the fracture face resulting in elevated frac fluid saturations within 2 – 6 inches of the frac face. Drainage and imbibitions capillary pressure analysis indicate that these saturations are not in equilibrium and capillary forces act to imbibe the fluid back into the reservoir away from the frac face over a period of weeks to months and can be slowed or halted by gas pressure decrease associated with well production. The frac fluids imbibed into the formation are effectively locked in place by capillary pressure forces of hundreds to thousands of pounds per square inch (psi) both during the life of the well production and for geologic periods of time after reservoir depletion. Further research is needed and is ongoing as to the exact shape of the imbibition capillary pressure curves and imbibition water relative permeability curves to fully quantify the imbibitions process and timing.

Selected References

Barree, R.D., Cox, S.A., Gilbert, J.V., and Dobson, M.: "Closing the Gap: Fracture Half Length from Design, Buildup, and Production Analysis," SPE 84491, *Proc.* 2003 SPE Annual Technical Conference and Exhibition, Denver, Colorado, 5-8 October.

Barree, R.D, 1983, “A Practical Numerical Simulator for Three Dimensional Fracture Propagation in Heterogeneous Media,” SPE 12273, presented at the 1983 SPE Symposium on Reservoir Simulation, San Francisco, CA, Nov. 15-18, 12 pgs.

Byrnes, A.P., and R.M. Cluff, 2009, “Analysis of Critical Permeablity, Capillary Pressure and Electrical Properties for Mesaverde Tight Gas Sandstones from Western U.S. Basins”, Final Report, U.S. Department of Energy contract #DE-FC26-05NT42660, 355 pgs.

Cipolla, C., X. Weng, M. Mack, U. Ganguly, H. Gu, O. Kresse, and C. Cohen, 2011, “Integrating Microseismic Mapping and Complex Fracture Modeling to Characterize Fracture Complexity,” SPE 140185-MS, SPE Hydraulic Fracturing Technology Conference, 24-26 January 2011, The Woodlands, Texas, USA, 22 pgs.

Fisher, M.K., Davidson, B.M., Goodwin, A.K., Fielder, E.O., Buckler, W.S., and N.P. Steinberger, 2002, “Integrating Fracture Mapping Technologies to Optimize Stimulations in the Barnett Shale,” SPE 77411-PA_P, presented at the 2002 SPE Annual Technical Conference and Exhibition, San Antonio, Texas, USA, Sept 29-Oct 2, SPE Production and Facilities, May, p. 85-93,

Mayerhofer, M.J., and M.J. Economides, 1997, “fracture-Injection-test Interpretation: Leak-Off vs. Permeability, SPE 28562, SPE Production and Facilities, Nov., p. 231-236.

Meyer, B.R., Cooper, G.D., and S.G. Nelson, 1990, “Real-Time 3-D Hydraulic Fracturing Simulation: Theory and Field Case Studies,” SPE 20658-MS, Proc. SPE Annual Technical Conference and Exhibition, 23-26 September 1990, New Orleans, Louisiana, p. 417-432.

Miller, M.A., Jenkins, C., and R. Rai, 2010, “Applying Innovative production Modeling techniques to Quantifying fracture Characteristics, Reservoir properties, and Well Performance in Shale Gas Reservoirs,” SPE 139097, presented at 2010 SPE Eastern Regional Meeting, Morgantown, West Virginia, USA, Oct 12-14, 12 pgs.

Nolte, K.G., 1986, “A General Analysis of Fracturing Pressure Decline With Application to Three Models,” SPE Formation Evaluation, Dec., p. 571-583.

Nolte, K.G., Mack, M.G., and Lie, W.L.: “A Systematic Method of Applying Fracturing Pressure Decline : Part I,” SPE 25845, Proc., SPE Rocky Mountain Regional/Low Permeability Reservoirs Symposium, Denver (1993), p. 31-50.

Warpinski, N., 1988, “Dual Leak-off Behavior in Hydraulic Fracturing of Tight, Lenticular Sands,” SPE 18259, SPE Production Engineering, p. 243-252.